Frontiers in Scientific Research and Technology

Online ISSN: 2682-2970
Print ISSN: 2682-2962
http://fsrt.journals.ekb.eg

FSRT J 6 (2023) 97 - 107 10.21608/FSRT.2023.214550.1095

Reduced Graphene Oxide Doped Vanadium Pentoxide Films as Promising Photostabilizer

M. M. Abdelrazek, N. A. Gazouly, Y. A Sharaby, M. M. El-Desoky*

Department of Physics, Faculty of Science, Suez University, Suez,Egypt, 43518

ARTICLE INFO

Article history:
Received 31 May 2023
Received in revised form 22 June 2023
Accepted 25 June 2023
Available online 2 July 2023

Keywords
Nanocrystalline Vanadium pentoxide films,
Reduced Graphene oxide,
rGO; Sol-Gel,
Photostabilizer,
Optical properties.

ABSTRACT

Vanadium pentoxide (V_2O_5) films doped with reduced graphene oxide (rGO) were synthesized using sol-gel method in the form of $rGOx.V_2O_5.nH_2O$ (given x = 0.10, 0.20 and 0.35 mole%) and characterized using X-ray diffraction (XRD) and high-resolution transmission electron microscopy (HRTEM) and found matching with ICCD card number 00-040-1296. The average crystalline size for each rGO concentration was determined using the Scherrer equation and found to be decreasing from 4.9 nm to 3.2 nm with as rGO increases. The UV-Vis spectroscopic analysis revealed that the films endorse strong UV absorption in the region of 200 to 500nm, making them a potential option for solar cell photostabilizer applications. Absorption before and after irradiation at different exposure times were measured. The relative absorption for pure and doped samples were measured as a function of irradiation time and found the addition of rGO decreased the photo-degradation. The rate constants K and the half life time $t_{1/2}$ of photo-degradation were calculated and compared to pure sample using Grabchev and Bojinov equations. The novelty of this study lies in the characterization of rGO-doped vanadium pentoxide films as the evaluation of their photostabilizing properties. The results indicate the potential of rGO as a valuable additive for enhancing the stability and durability of photovoltaic devices, opening up new possibilities for future advancements in solar energy technologies

1. Introduction

Due to its crucial function in a variety of applications and energy-related technologies, the research of optical properties of diverse materials has become more and more important in recent years. Understanding these materials' optical characteristics is crucial for creating novel solutions to today's problems as well as for addressing present and future demands [1]. Electronics that are optically transparent are essential in modern technology, especially in energy-related applications like solar cells. Due to its unique optical characteristics, vanadium pentoxide produced via the sol-gel process is a potential material for various applications [2].

Vanadium pentoxide sol-gel, $V_2O_5.nH_2O$, has a special structure that allows water molecules to intercalate between its layers, according to a theory put forth by Aldebert [3].

The structural model for vanadium pentoxide, V_2O_5, as proposed by T. Yao and Y. Oka [4] has a lamellar structure, as shown in Figure 1 (a) and (b), respectively which is a distorted orthorhombic structure with a flat-sheet like shape. This structure is thought to be the primary reason for its distinctive optical properties and serves as a promising starting point for a wide range of combinations through doping materials that directly alter the structural and optical properties. Vanadium pentoxide can be intercalated by numerous transitional metals due to its layered structure, which changes or adds physical features. [5]. From previous work [6-8], the band gap of vanadium pentoxide is approximately 2.2eV which is suitable for photovoltaic application.

Photostabilizers are essential additives used to protect materials from the harmful effects of ultraviolet (UV) radiation, which can cause degradation and deterioration. Vanadium pentoxide (V_2O_5) is a well-known photostabilizer due to its ability to absorb and dissipate UV radiation. It is commonly used in the production of plastics, coatings, and other materials that are susceptible to degradation by UV radiation. V_2O_5 acts as a UV absorber, which means that it absorbs the harmful UV radiation and converts it into heat, thereby protecting the material from degradation. V_2O_5 is also known to have catalytic properties, which can further enhance its effectiveness as a photostabilizer . However, its performance can be further enhanced by doping it with

* Corresponding author at Suez University

E-mail addresses: mmdesoky@gmail.com (M. M. El-Desoky)

reduced graphene oxide (rGO), a promising nanomaterial with excellent properties. The combination of V_2O_5 sol gel and rGO can lead to a novel photostabilizer with improved efficiency, stability, and durability.

Sol gel is a versatile and widely used method for synthesizing V_2O_5 nanoparticles with controllable size, morphology, and structure. It involves the hydrolysis and condensation of precursor molecules to form a colloidal suspension, which can be further processed to obtain solid materials. Doping V_2O_5 sol gel with rGO can be achieved by dispersing rGO sheets into the sol gel precursor solution during the synthesis process, allowing rGO to be uniformly distributed in the resulting V_2O_5 matrix. Reduced graphene oxide (rGO) is a graphene derivative that is obtained by chemically reducing graphene oxide, a graphene precursor. rGO exhibits unique properties, such as high surface area, excellent electrical conductivity, and strong mechanical strength. These properties make rGO an ideal candidate for enhancing the performance of V_2O_5 as a Photostabilizer [9]. The doping of V_2O_5 sol gel with rGO can lead to several beneficial effects. First, rGO can act as a sensitizer, effectively absorbing UV radiation and transferring the energy to V_2O_5, thereby enhancing its photo-stabilizing capability. Second, rGO can provide additional stability to the V_2O_5 matrix, preventing aggregation and improving the dispersion of V_2O_5 nanoparticles, which can result in better performance and longer durability. Third, the electrical conductivity of rGO can facilitate charge transfer and separation in the V_2O_5 matrix, leading to improved photostability performance [10].

This paper aims to investigate the effects rGO on the photostability characteristics of nanocrystalline vanadium pentoxide films for solar cells and opto-electronic applications. The samples were prepared via sol-gel technique in the form of $rGO_xV_2O_5.nH_2O$ (where x= 0.10, 0.20 and 0.35 mol%).

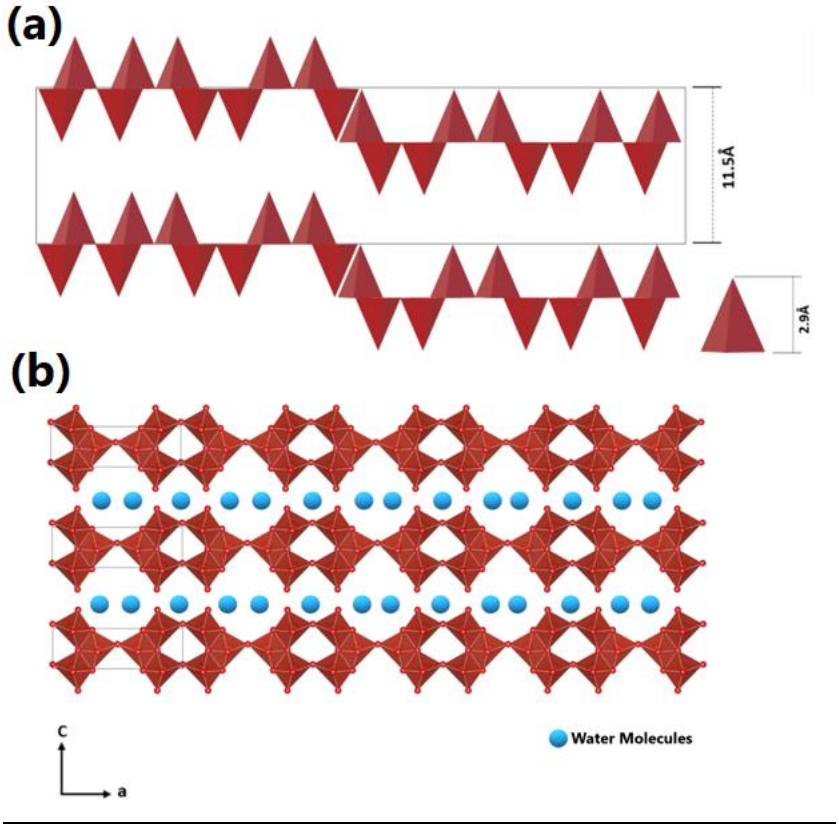

Figure 1 (a) Structural model for theV_2O_5 layers, proposed by Aldebertetal, and (b) Structural model for theV_2O_5 xerogel, proposed by Yao etal

2. Experimental

Both Graphite and Vanadium pentoxide (V_2O_5) powders were purchased in 99.9% purity from Sigma-Aldrich. Modified Hummer method [11, 12], was used to prepare reduced graphene oxide (rGO). Three different doping concentrations of rGO are used to prepare samples in the form $rGO_x.V_2O_5.nH_2O$ (where x = 0.10, 0.20 and 0.35 mol%). The prepared doping of rGO is prepared in DW and kept in sonication for 1hr to assure homogeneity of the rGO sheets. A 30ml of 25% hydrogen peroxide, H_2O_2 is prepared under stirring. Following which, while stirring, add 1g of pure V_2O_5 and an exothermic reaction begins indicating the readiness for gel formation. Then, within 15 minutes of medium stirring, and before gelation starts, the prepared doping of rGO is

added to assure intercalation of rGO into the layers of vanadium pentoxide. After gelation, dip-coating method is used for each concentration to prepare thin films , as shown in Figure 2. The coating procedure begins at a predetermined time of 5 hours after the reaction to ensure uniform viscosity. The coating is applied in a single coating layer at room temperature with an average withdrawal speed of 15 mm/s.

For structural study, XRD and HRTEM are used. For XRD, Siemens / Bruker D5000 X-ray Diffractometer (powered with monochromatic Cu-Kα radiation source with wavelength of λ = 1.5406 Å). Test was carried against 2Θ varying from 5 to 60 degrees with a 0.05-degree step. The resulted graphs are processed and analyzed for peaks pattern recognition using X'Pert HighScore® software to identify the closed match card in ICDD library. Then, using Origin ® -grapher and analysis software, the main peak's full width half maximum (FWHM) is used to with Scherrer equations to calculate average crystallite size. For HRTEM, JEOL JEM-2100 high resolution transmission electron microscopy (HRTEM), which is fitted with a lanthanum hexaboride LaB6 electron gun operating at 200 kV and measures particle size at a scale of 50 nm. Selected area diffraction (SAD) is used to for calculating d-spacing.

The METASH 9000 UV/VIS spectrophotometer, operating from UV region (190 nm) to the IR region (1100 nm), was used to measure the optical characteristics. The produced samples were examined at room temperature for optical transmittance (T), absorption (A), and reflectance (R). The base line is automatically adjusted before any set of measurements using the slit width or signal amplification gain. We used a 400W TOKINNA JTT halogen lamp as the light source for the irradiation. The sample was exposed to various times for each of the chosen rGO% concentrations, and at each exposure time, the absorption spectra were measured.

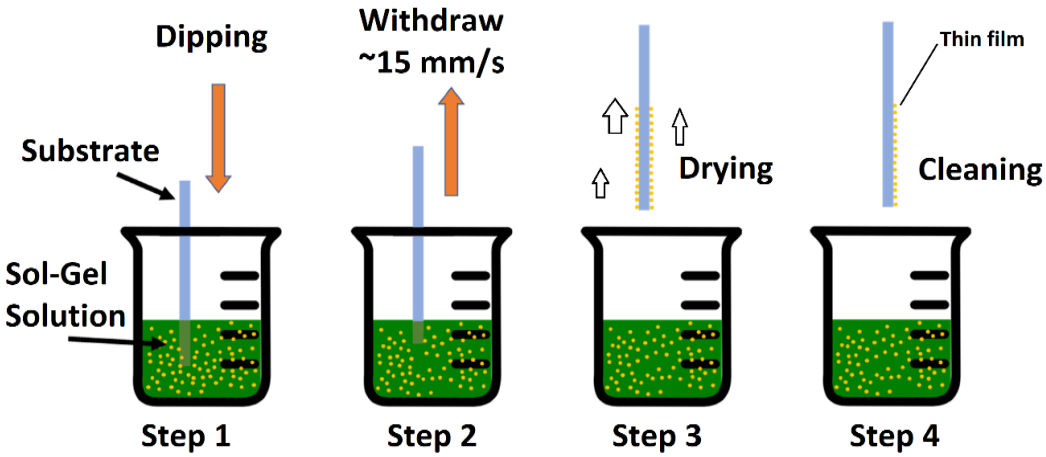

Figure 2 Dip coating illustration

3. Results and discussion

3.1. Structural analysis by XRD and HRTEM

Figur**e 3** shows the acquired XRD patterns of the generated $rGOxV_2O_5.nH_2O$ films for various rGO concentrations. It exhibits four primary peaks that are consistent with the card number 00-040-1296 or/and (JCPDS 40-1296) of vanadium pentoxide xerogel with orthorhombic crystal structure (001), (003), (004), and (005) [13, 14]. The resultant structure can be characterised as nanocrystalline of highly aligned nanocrystals twoard c-axis from the examination of XRD peaks [15]. For the various doppings of rGO, the primary peak (001) is observed to be virtually fixedly located at 2Θ = 6.8~7.2.

Due to the preparation conditions and layer structure of the nanocrystalline films, the pure V_2O_5 sample at 2Θ ≈ 12 exhibits the line from the (002) plane with weak intensity. This line becomes weaker and eventually disappears as the rGO concentration rises from 0.10 to 0.35 mol%, which is explained by the intercalation of rGO within the V_2O_5 layers. With the addition of rGO%, it is discovered that the intensity of the primary peak (001) is diminishing, indicating a level of intercalation that affects the crystallite size. With their c-axis normal to the substrate surface, the resulting nanocrystalline films were confirmed to be strongly oriented nanocrystals using XRD examination [15].

Scherrer equation, Eq. (1) is used to calculate the average particle size (D) of nanocrystalline films:

$$D = \frac{k\lambda}{\beta \cos\theta} \quad (1)$$

k is a factor related to the particles shape (k ≈1), the wavelength, λ= 1.5406 Å for Cu (kα), β is the full width at half maximum (FWHM) and Θ is Bragg's angle [16]. For the primary peaks (001) & (003), we applied the Lorentzian fitting method in the Origin® software to obtain the (FWHM), which allowed us to determine the average crystalline size as listed in Table 1.

.

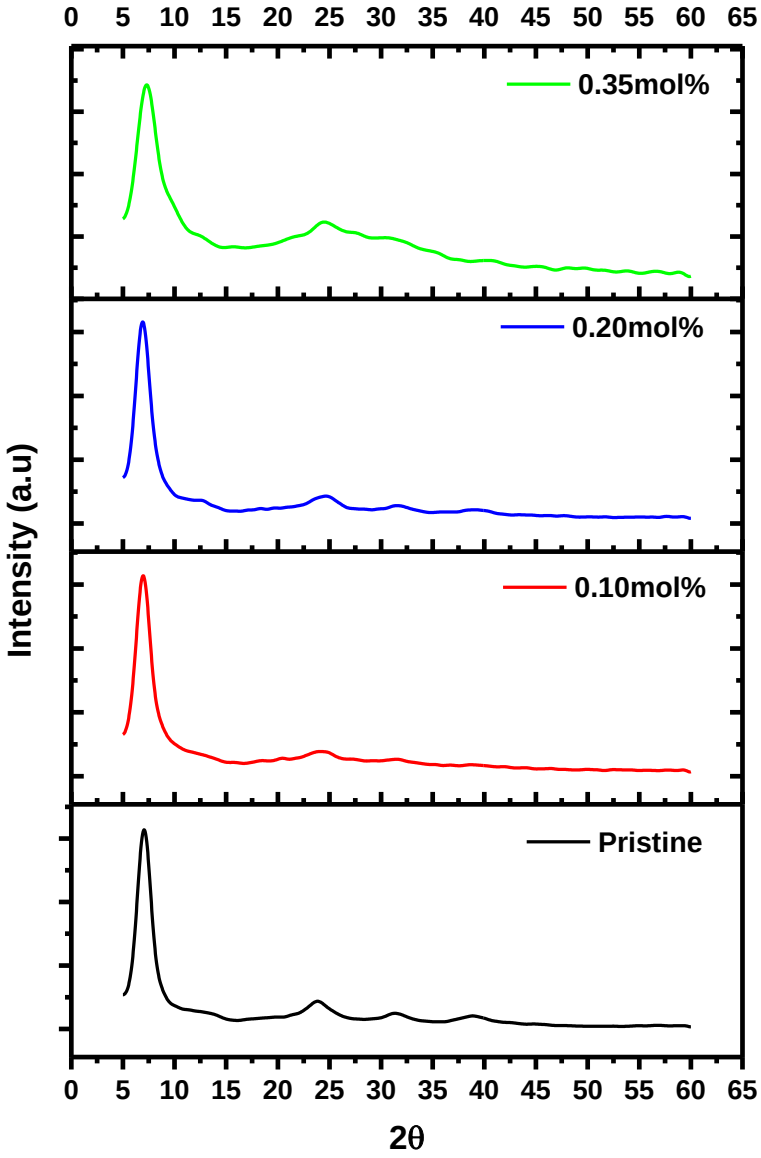

Figure 3 Room-temperature XRD for different rGO concentrations

Table 1 Average crystalline size, Rate constants K and the half life time $t_{1/2}$ of photo-degradation for different rGO concentration

rGO mol%	Average D	k $(min)^{-1}$	$t_{1/2}$ (min)
0	4.9	0.000762	910
0.10	4.11	0.000709	977
0.20	3.83	0.000118	5900
0.35	3.2	-0.0000308	-22500

As indicated, the addition of rGO reduced the average crystalline size from 4.9 nm to 3.2 nm which can be attributed to the increase of internal stress caused by the doping [8].

High resolution transmission electron microscopy (HRTEM) observation provides the structural data of the generated samples with rGO of 0.10 mol%, 0.20 mol%, and 0.35 mol%. Figure 4 displays general view HRTEM images for rGO concentrations of 0.10 mol%, 0.20 mol%, and 0.35 mol% at various scales up to 1 µm. The vanadium particles are pierced by rGO soot that is over 1000 nm (1 µm) broad compared to pure V_2O_5 with no rGO, demonstrating the successful fabrication of rGO sheets inserted into vanadium layers.

The particle size was determined at a scale of 50nm, as shown in Figure 5, where clustered particles ranged in size from 4.5nm to 33nm. The small single particles with a size between 4 and 6 nm are consistent with the average crystalline size predicted from XRD observations, and can therefore be regarded expected.

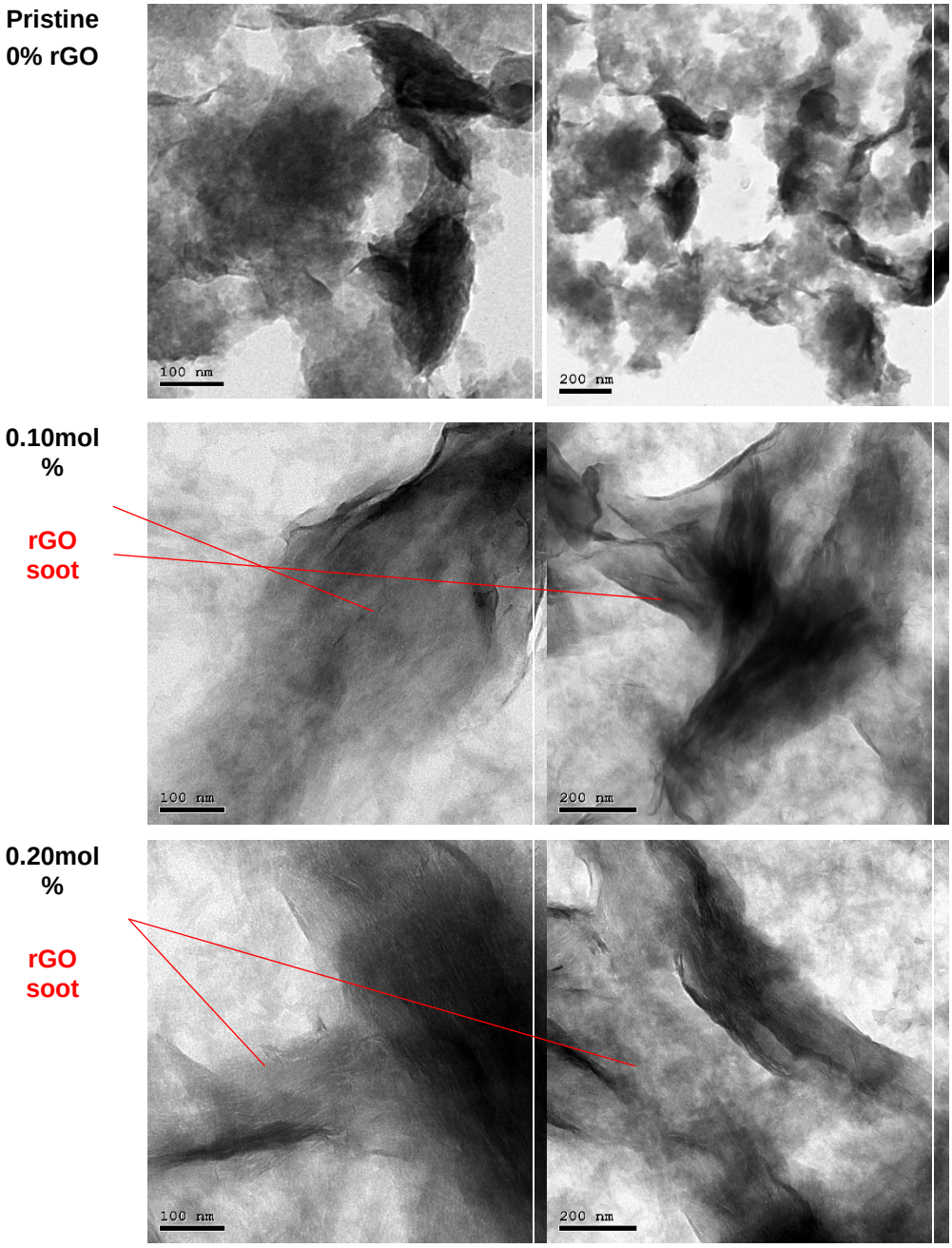

Figure 4 General structural view at 100nm and 200nm scales showing rGO soot in doped samples

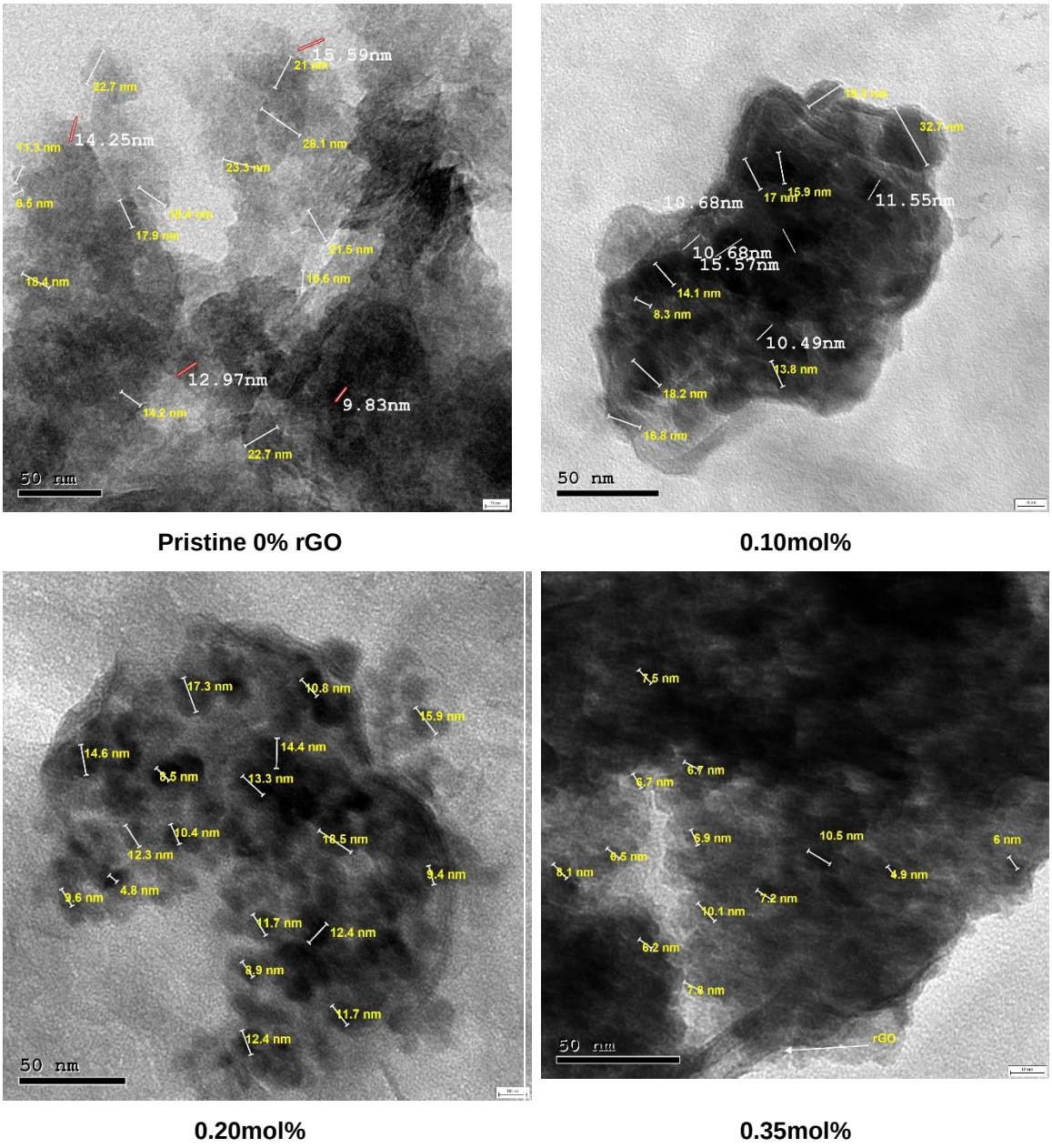

Pristine 0% rGO **0.10mol%**

0.20mol% **0.35mol%**

Figure 5 Particle size measured at 50nm scale for different rGO concentrations

3.2. UV- visible spectroscopic analysis

Figure 6a, b, and c, respectively, show the absorption, reflectance and transmittance spectra as functions of wavelength in the range of 200 to 1200 nm, which were measured at room temperature. In Figure 6(a), the absorptivity drops from 200 to 500 nm as the rGO increases, although wave lengths below 500 nm do not change. This suggests strong UV absorption, making it a potential option for solar cell photostabilizer applications [17–19]. Multi-layered graphene has lower absorption intensity than single and double layers, which is thought to be the cause of the drop in absorption following the addition of rGO [20].

Figure 6 (b) demonstrates that when rGO content increases, reflectance generally falls, particularly in the lower wavelength area up to 500 nm. As seen in earlier works [17-19], this overlapping behaviour is characteristic for vanadium pentoxide nanocrystalline films. The tendency of reflectance to decrease with the addition of rGO is connected to the rise in the number of layers of rGO, but it also decreases with the replacement of high-reflectance V_2O_5 with low reflectance rGO [20].

On the other hand, the addition of low-absorbing rGO and the replacement of high-absorbing V_2O_5 with high-transparent rGO material (~ 97.7% transperent) and hence decreases absorption [21]. The transmittance spectrum in Figure 6 (c) may also be separated into two regions: from 200 to 500 nm, the transmittance rises as rGO increases, whereas from 500 to 1200 nm, the transmittance falls as rGO rises. Additionally, the region

between 500 and 1200 nm has a usually higher transmittance than the region between 200 and 500 nm. This characteristic demonstrates that the addition of rGO can be used to regulate transmittance for specific wavelengths.

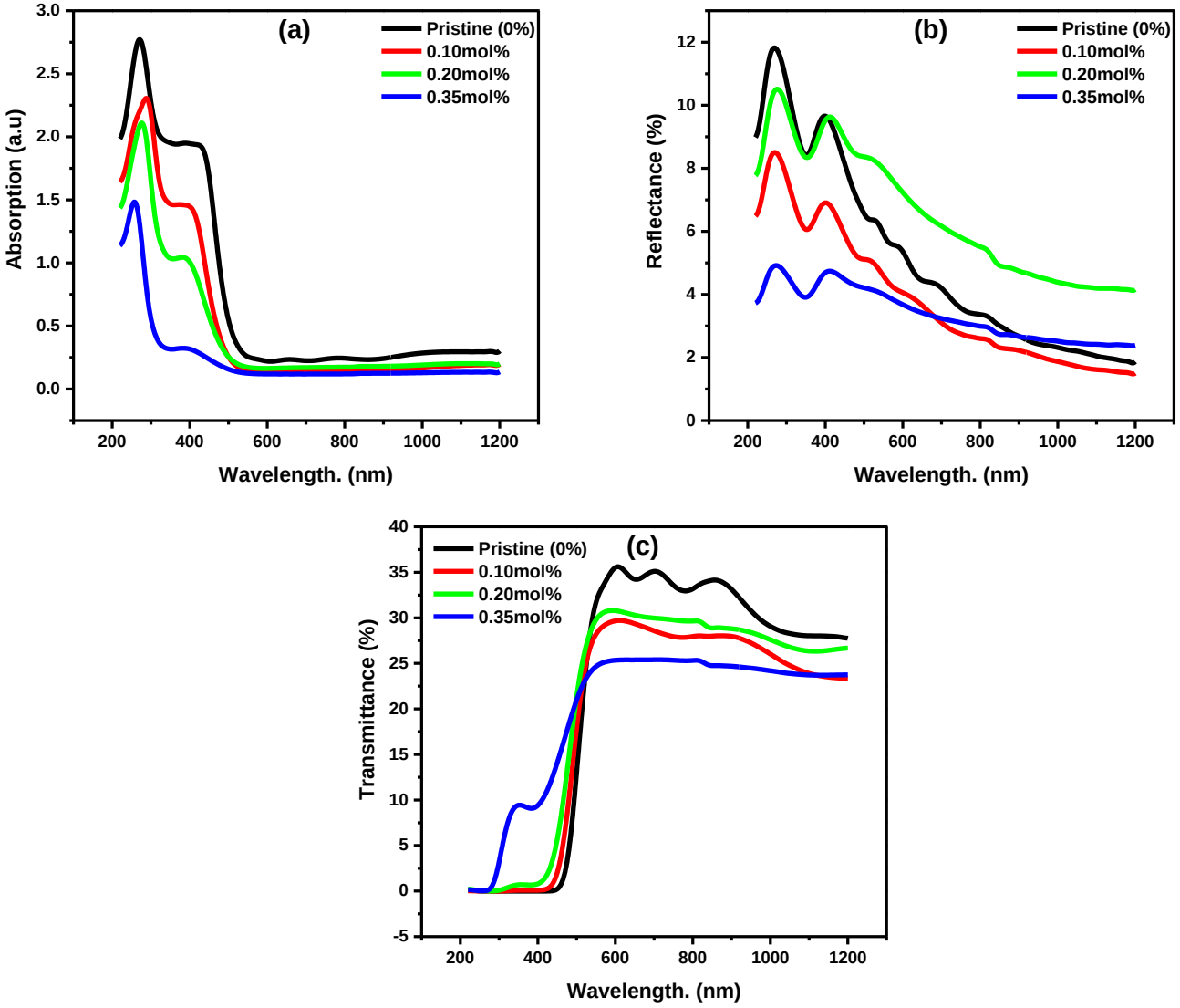

Figure 6 (a) Absorption, (b) Reflectance and (c) Transmittance for different rGO concentration

3.3. Application for $rGOxV_2O_5.nH_2O$ nanocrystalline films as Photostabilizer.

The absorption of light in a solar cell is not constant over time. As light irradiation of UV causes degeneration in the absorption layer which reduces the efficiency of the photoelectric process. The ability of a solar cell to maintain high absorption of light over time is called photostability. Photostability, or stability under light irradiation, is one of the main obstacles affecting the performance of solar cells. As the prepared $rGOxV_2O_5.nH_2O$ nanocrystalline films showed high absorption in the range 200 to 500 nm as indicated In Figure *7*(a) with good absorption in the UV region. This is a promising candidate for solar cell photostabilizer applications [22-24].

In the following paragraphs the photostability of the prepared $rGOxV_2O_5$ nH_2O nanocrystalline films will be studied. Samples were chosen for rGO= 0% (pure), 0.10 mol%, 0.20 mol% and 0.35 mol%

3.3.1 Absorption before and after irradiation

Absorption for selected samples was measured before and after UV-visible-IR irradiation with 400-watt tungsten lamp. Figure *7*(a-d) illustrates the absorption before and after irradiation at different times up to 4hrs for samples with rGO= 0% (pure), 0.10 mol%, 0.20 mol% and 0.35 mol% respectively.

In Figure *7*(a), absorption pure sample (rGO=0 mol%), decreases with increasing exposure time due to degeneration process. The phenomenon is observed in 0.10 mol% rGO as in Figure *7*(b). But in Figure *7*(c) with rGO of 0.20%, the absorption after 1hr increases relative

to absorption before irradiation which can be attributed to extension in the reduction process of some partially reduced graphene oxide to completely reduced graphene oxide [25, 26]. However, increasing exposure time up to 3hrs, the absorption decreased to the initial level before exposure. Then the absorption decreases after exposure to 4hrs.

For higher rGO content in rGO=0.35 mol% as illustrated in Figure 7(d), the same behavior noted similar to 0.20mol% but with much lower divergence over exposure time. The divergence for each rGO concentration can be studied by relative absorption.

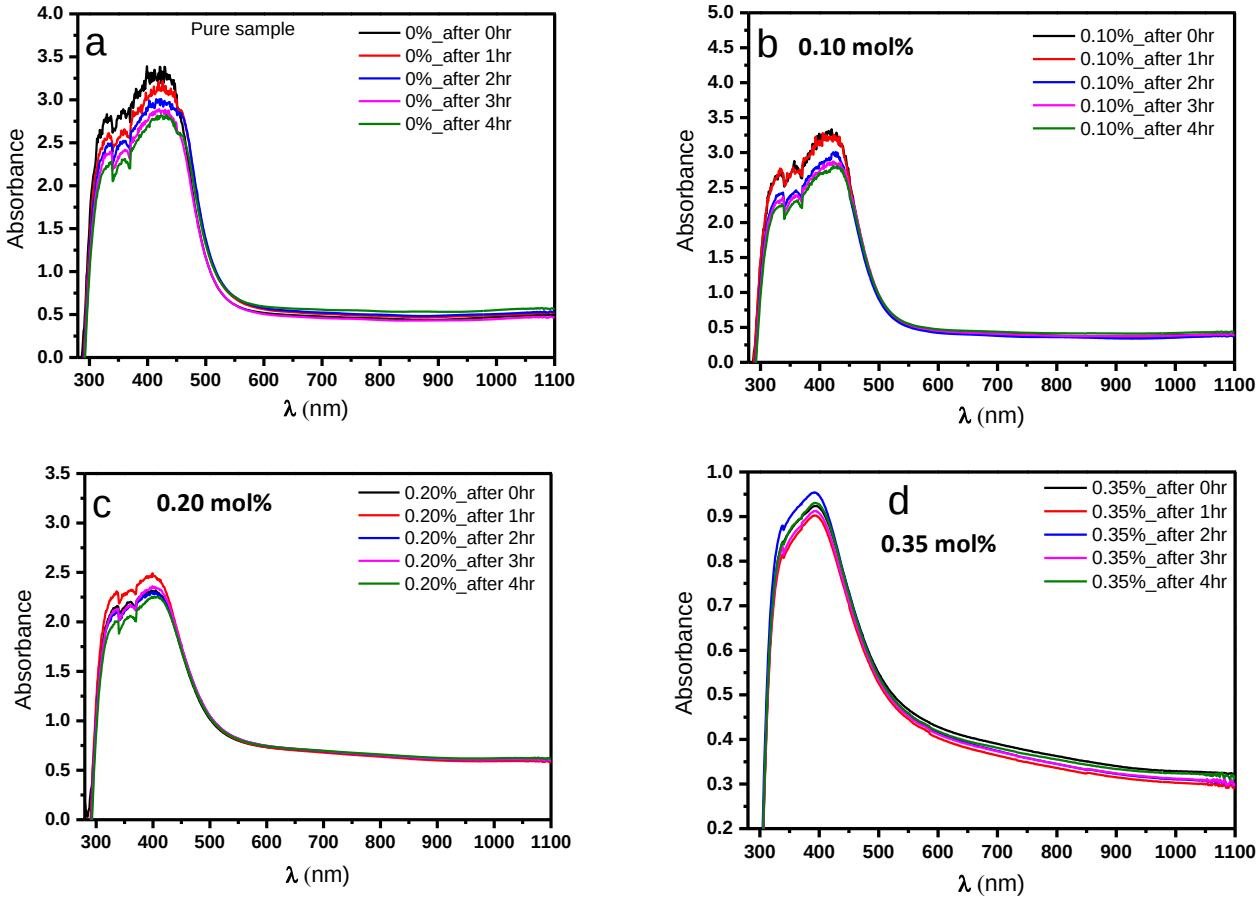

Figure 7 (a-d) Absorption before irradiation (after 0hrs) and after irradiation at different exposure time up to 4hrs for different rGO concentration

3.3.2 Relative absorption before and after irradiation

Relative absorption, or (A/A_o % where A_o is measured absorption before irradiation and A is measured absorption after irradiation) for selected samples was measured study the divergence in absorption as a function of irradiation time for each rGO concentration. Figure 8 illustrates the relative absorption for selected rGO as a function of irradiation time. The degeneration process can be identified as a decrease in the relative absorption as indicated in the pure sample and rGO of 0.10mol%. But in the samples with higher rGO concentration (0.20mol% and 0.35mol%), the relative absorption is increasing with some reading above 100%. For sample with 0.35 mol% rGO, the average relative absorption is 98.9% as measured by line fitting as indicated in Figure 8 which exhibits good stability under UV-visible-IR irradiation.

3.3.3 Rate constants and the half life time

The rate constant K (or reaction rate) represent the rate of photodegradation due to exposure. And the half-life time $t_{1/2}$ is the time needed for the photodegradation process to affect the absorption to be reduced to 50% from its initial value.

To examine the rate constants K and the half life time $t_{1/2}$ of photo-degradation of selected samples, the following Eq. (2) and Eq. (3) according to Grabchev and Bojinov was used [27] and illustrated in Table 1.

$$K = \frac{2.303}{t} \log \frac{A_o}{A} \quad (2)$$

$$t_{1/2} = \frac{0.693}{k} \quad (3)$$

Where A_o is measured absorption before irradiation and A is measured absorption after irradiation and t is the time of exposure in minutes. Rate constants K and the half life time $t_{1/2}$ of photo-degradation of rGO_x V_2O_5 nH_2O nanocrystalline films.

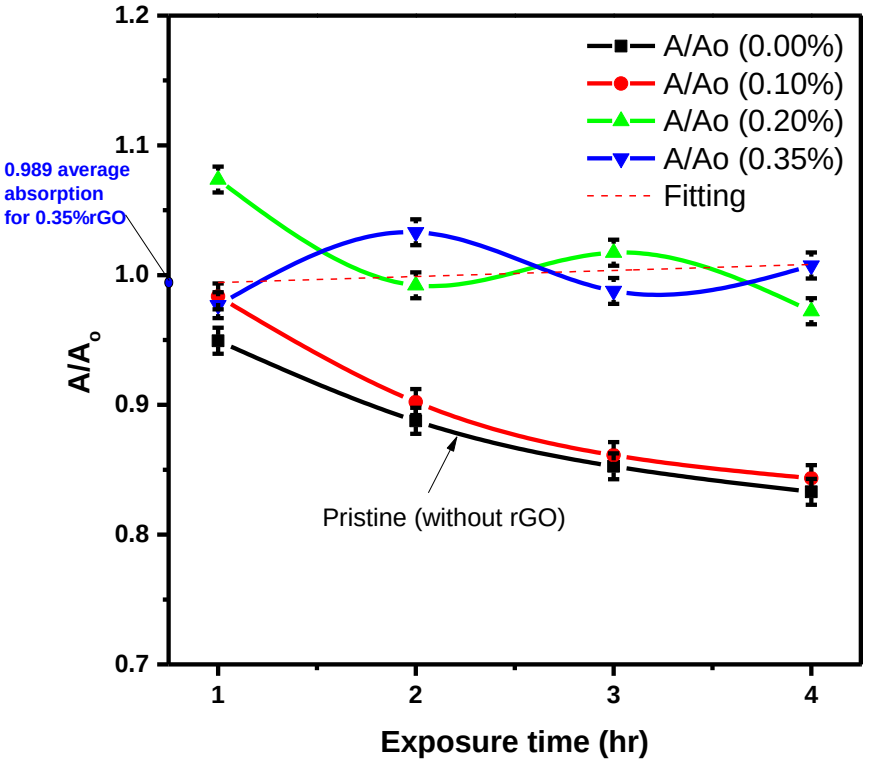

Figure 8 Relative absorption for different rGO concentration as a function of irradiation time

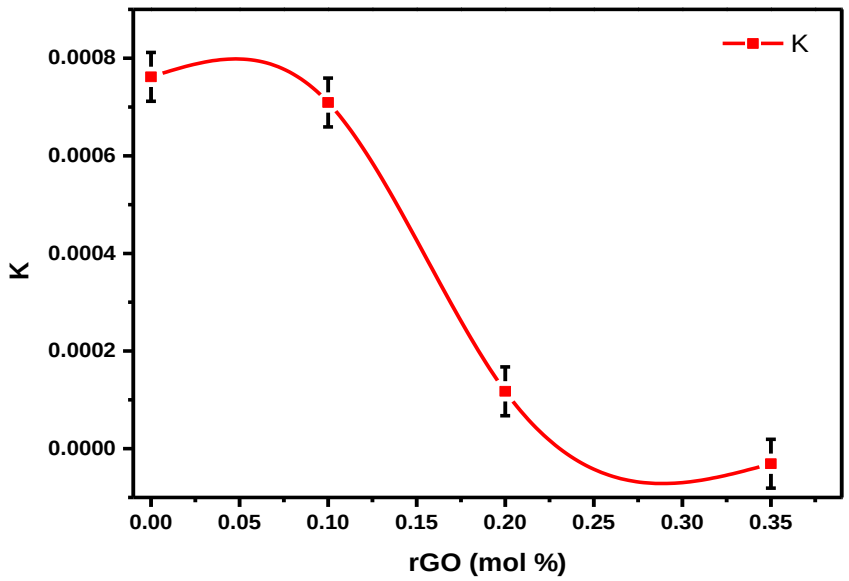

Figure 9 Rate constants K of photo-degradation for different rGO concentration

Figure 9 and Figure 10 illustrate rate constants K and the half life time $t_{1/2}$ respectively for photo-degradation of rGOx V_2O_5 nH_2O nanocrystalline films after 4hrs of exposure. From Figure 9 , the effect of rGO is clearly reducing the photodegradation as the rate constants K is decreasing with the increasing of rGO.

The half-time $t_{1/2}$ illustrated in Figure 10 increases by the increase of rGO which indicates that rGO will increase the stability time of the absorption process as the photodegradation process will take longer. For the pure sample, it would take about 900 min (or about 15 hrs) for the photodegradation process to cause absorption reduction by 50% from its initial value, but for 0.20% rGO, it would take about 5900 min (or about 98 hrs) to reach the same level. When increasing the rGO to 0.35%, the absorption is higher than int's initial state as illustrated in Fig 8 which will yield a negative half-time value indicating almost no degradation at this concentration of rGO.

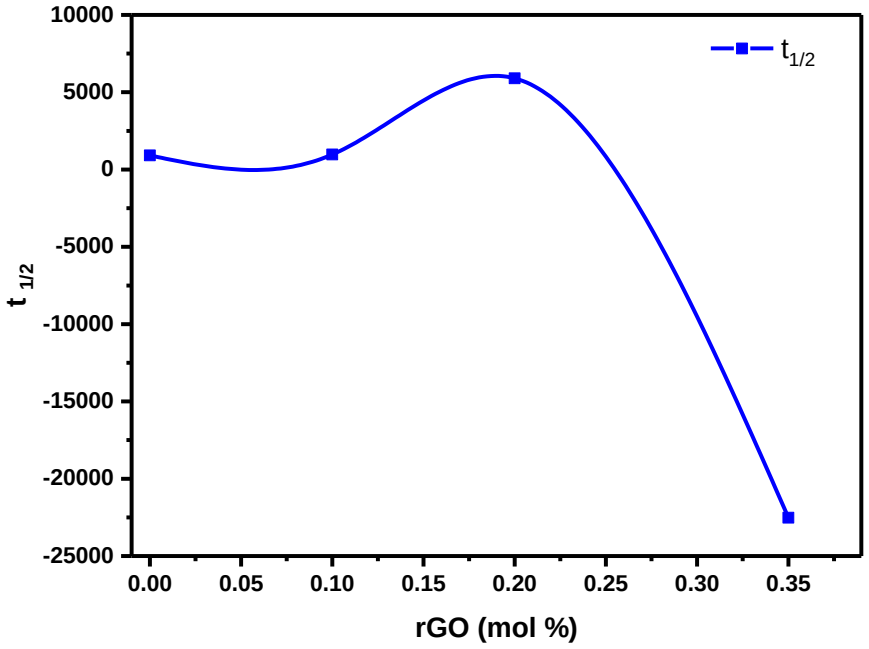

Figure 10 Half-life time $t_{1/2}$ of photo-degradation for different rGO concentration

4. Conclusion

The sol-gel technique was used to create nanocrystalline thin films of $rGOxV_2O_5.nH_2O$ ($0 \leq x \geq 0.35$). The structural analysis by XRD and HRTEM showed that the addition of reduced graphene oxide (rGO) to vanadium pentoxide (V_2O_5) films resulted in a decrease in crystalline size from 4.9 nm to 3.2 nm, as determined by the Scherrer equation. HRTEM observations showed that rGO sheets were successfully inserted into the V_2O_5 layers, with particle sizes ranging from 4.5 nm to 33 nm. UV-visible spectroscopic analysis revealed that the addition of rGO affected the absorption, reflectance, and transmittance properties of the films. The absorptivity dropped from 200 to 500 nm as the rGO concentration increased, while wavelengths below 500 nm remained constant. This suggests strong UV absorption, making the films a promising candidate for solar cell photostabilizer applications. The reflectance generally decreased with increasing rGO content, particularly in the lower wavelength area up to 500 nm, while the transmittance increased from 200 to 500 nm and decreased from 500 to 1200 nm. The region between 500 and 1200 nm had a higher transmittance than the region between 200 and 500 nm, demonstrating that the addition of rGO could be used to regulate transmittance for specific applications. Overall, the prepared samples of rGOxV_2O_5 nH_2O nanocrystalline films showed a promising application as a photo-stabilizer for solar cells and optical sensors as the effect of adding reduced graphene oxide rGO was proven to be excellent inhibitor for the photo-degradation process in the range from 300 to 1100 nm.

References

[1] P. Capper, A. Willoughby, and S. O. Kasap, *Optical Properties of Materials and Their Applications*. John Wiley & Sons, 2020.

[2] E. Prociow, M. Zielinski, K. Sieradzka, J. Domaradzki, and D. Kaczmarek, "Electrical and optical study of transparent V-based oxide semiconductors prepared by magnetron sputtering under different conditions," *Radioengineering,* vol. 20, no. 1, pp. 204-208, 2011.

[3] J.-J. Legendre, P. Aldebert, N. Baffier, and J. Livage, "Vanadium pentoxide gels:: II. Structural study by x-ray diffraction," *Journal of Colloid and Interface Science,* vol. 94, pp. 84–89, 07/01 1983.

[4] T. Yao and Y. Oka, "On the layer structure of vanadium pentoxide gels Comment on “Molecular dynamic simulation of the vanadium pentoxide gel host”," *Solid state ionics,* vol. 96, no. 3-4, pp. 127-128, 1997.

[5] Z. Mohaghegh, F. E. Ghodsi, and J. Mazloom, "Comparative study of electrical parameters and Li-ion storage capacity of PEG modified β-V_2O_5: M (M: Mo, Ni) thin films," *Journal of Materials Science: Materials in Electronics,* vol. 30, pp. 13582-13592, 2019.

[6] M. M. El-Desoky, M. M. Abdulrazek, and Y. A. Sharaby, "Characterization and optical properties of reduced graphene oxide doped nano-crystalline vanadium pentoxide," *Optical and Quantum Electronics,* vol. 52, no. 6, p. 315, 2020/06/06 2020.

[7] M. M. El-Desoky, M. M. Abdulrazek, and Y. A. Sharaby, "Fabrication and electrical properties of reduced graphene oxide doped nanocrystalline vanadium pentoxide films," *Materials Science and Engineering: B,* vol. 261, p. 114676, 2020.

[8] M. M. Abdelrazek, A. E. Hannora, R. M. Kamel, I. Morad, and M. M. El-Desoky, "Effect of lanthanum doping on the structure and optical properties of nanocrystalline vanadium pentoxide films prepared by sol–gel method," *Optical and Quantum Electronics,* vol. 55, no. 6, p. 491, 2023/04/08 2023.

[9] S. Karimi *et al.*, "A review on graphene’s light stabilizing effects for reduced photodegradation of polymers," *Crystals,* vol. 11, no. 1, p. 3, 2020.

[10] S. R. Pathipati, E. Pavlica, E. Treossi, V. Palermo, and G. Bratina, "The role of charge transfer at reduced graphene oxide/organic semiconductor interface on the charge transport properties," *Organic Electronics,* vol. 77, p. 105499, 2020/02/01/ 2020.

[11] N. I. Kovtyukhova *et al.*, "Layer-by-layer assembly of ultrathin composite films from micron-sized graphite oxide sheets and polycations," *Chemistry of materials,* vol. 11, no. 3, pp. 771-778, 1999.

[12] W. S. Hummers Jr and R. E. Offeman, "Preparation of graphitic oxide," *Journal of the american chemical society,* vol. 80, no. 6, pp. 1339-1339, 1958.

[13] M. Al-Assiri, M. El-Desoky, A. Alyamani, A. Al-Hajry, A. Al-Mogeeth, and A. Bahgat, "Spectroscopic study of nanocrystalline $V_2O_5 \cdot nH_2O$ films doped with Li ions," *Optics & Laser Technology,* vol. 42, no. 6, pp. 994-1003, 2010.

[14] Z. Li, H. Sun, J. Xu, Q. Zhu, W. Chen, and G. S. Zakharova, "The synthesis, characterization and electrochemical properties of $V_3O_7 \cdot H_2O$/CNT Nanocomposite," *Solid State Ionics,* vol. 262, pp. 30-34, 2014.

[15] A. Bahgat, F. Ibrahim, and M. El-Desoky, "Electrical and optical properties of highly oriented nanocrystalline vanadium pentoxide," *Thin Solid Films,* vol. 489, no. 1-2, pp. 68-73, 2005.

[16] E. F. Kaelble, "Handbook of X-rays: for diffraction, emission, absorption, and microscopy," *McGraw-Hill, New York,* pp. 17.1-17.18, 1967. McGraw-Hill

[17] F. Dultsev, L. Vasilieva, S. Maroshina, and L. Pokrovsky, "Structural and optical properties of vanadium pentoxide sol–gel films," *Thin Solid Films,* vol. 510, no. 1-2, pp. 255-259, 2006.

[18] M. Abyazisani, M. M. Bagheri-Mohagheghi, and M. R. Benam, "Study of structural and optical properties of nanostructured V_2O_5 thin films doped with fluorine," *Materials Science in Semiconductor Processing,* vol. 31, pp. 693-699, 2015.

[19] N. M. Tashtoush and O. Kasasbeh, "Optical properties of vanadium pentoxide thin films prepared by thermal evaporation method," *Jordan Journal of Physics,* vol. 6, pp. 7-15, 2013.

[20] B. G. Ghamsari, J. Tosado, M. Yamamoto, M. S. Fuhrer, and S. M. Anlage, "Measuring the complex optical conductivity of graphene by fabry-pérot reflectance spectroscopy," *Scientific reports,* vol. 6, pp. 1-6, 2016.

[21] D. A. Brownson, D. K. Kampouris, and C. E. Banks, "Graphene electrochemistry: fundamental concepts through to prominent applications," *Journal of Chemical Society Reviews,* vol. 41, no. 21, pp. 6944-6976, 2012.

[22] S.-W. Lee *et al.*, "UV degradation and recovery of perovskite solar cells," *Scientific reports,* vol. 6, pp. 1-10, 2016.

[23] B. Roose *et al.*, "Mesoporous SnO_2 electron selective contact enables UV-stable perovskite solar cells," *Journal of Nano Energy,* vol. 30, pp. 517-522, 2016.

[24] B. Roose *et al.*, "A Ga-doped SnO_2 mesoporous contact for UV stable highly efficient perovskite solar cells," *Journal of Materials Chemistry,* vol. 6, no. 4, pp. 1850-1857, 2018.

[25] Z. Ding, Z. Hao, B. Meng, Z. Xie, J. Liu, and L. Dai, "Few-layered graphene quantum dots as efficient hole-extraction layer for high-performance polymer solar cells," *Nano Energy,* vol. 15, pp. 186-192, 2015.

[26] J. Liu, Y. Xue, Y. Gao, D. Yu, M. Durstock, and L. Dai, "Hole and electron extraction layers based on graphene oxide derivatives for high-performance bulk heterojunction solar cells," *Advanced Materials,* vol. 24, no. 17, pp. 2228-2233, 2012.

[27] I. Grabchev, V. Bojinov, and stability, "Synthesis and characterisation of fluorescent polyacrylonitrile copolymers with 1, 8-naphthalimide side chains," *Polymer degradation,* vol. 70, no. 2, pp. 147-153, 2000.